Journal of Electroanalytical Chemistry 836 (2019) 176–181

Contents lists available at ScienceDirect

Journal of Electroanalytical Chemistry

journal homepage: www.elsevier.com/locate/jelechem

Polarization model of microbial fuel cell for treatment of actual potato chips processing wastewater associated with power generation

Ahmed Y. Radeef, Zainab Z. Ismail*

Department of Environmental Engineering, University of Baghdad, Baghdad, Iraq

ARTICLE INFO

Keywords:
Microbial fuel cell
Modeling
Electricity generation
Food processing wastewater

ABSTRACT

A dual chamber-microbial fuel cell (MFC) was used for simultaneous biotreatment of actual potato chips processing wastewater and electricity generation. The results demonstrated high removal efficiency of COD up to 90% after 14 days of continuous operation with 95.7 mW/m^2 power density at the closed circuit. An electrochemical model which describes the effect of various parameters on the performance of MFC was proposed to obtain the cell polarization. The results indicated the validity of the suggested model to create polarization curve with coefficients of determination (R^2) of 0.99, 0.92 and 0.92 for current, power densities, and voltage, respectively.

1. Introduction

The potato processing industries including potato chips processing industry present a serious of water pollution problems because these industries normally consume about 230 million liters of water required for processing 13,600 tons of potato in different processing steps. Furthermore, the potato processing wastewater contains high concentrations of proteins and starch which are biodegradable components, in addition to high concentrations of total suspended solids (TSS), chemical oxygen demand (COD), and total kjeldahl nitrogen (TKN). Raw potato processing wastewaters may contain up to 10,000 mg/L COD. Volatile suspended solids and total suspended solids can also reach 9500 and 9700 mg/L, respectively [1].

On the other hand, microbial fuel cell (MFC) is a new emerging bio-electrochemical technology for simultaneous treatment of organic-loading wastes and electricity generation. MFCs utilize the electro-active bacteria as biocatalysts for the reduction and/or oxidation reactions of the organic matters in the wastewater [2]. Microbial fuel cell (MFC) is a complex system in which a chemical signal is converted into an electrical signal. Due to the importance of developing more efficient engineering design of MFCs or for a better understanding the mechanisms of bio-electrochemical processes in the MFC, various modeling and simulation studies have been developed in this regard. The performance of the microbial fuel cells can be characterized based on the polarization curve which can be obtained by plotting the potential of cell versus current (or current density). The polarization curves firmly depend on numerous operational variables of the energy cell, such as temperature, relative humidity, pressure, current, and flow rate [3]. Therefore, the image of any fuel cell is the polarization curve, which represents how much of the open-circuit potential has to be spent to generate a given current. Normally, measuring the polarization curve is performed as a first step of the cell characterization [4]. Marcus et al. [5] considered the application of electrochemical reactions model in the MFC based on the mass transfer, Ohm law, and Nernst–Monod kinetic model with the direct conduction of electrons in biofilm. Picioreanu et al. [6] investigated the effects of culture suspended growth on the anode surface in one, two, and three dimensions' models. Zeng et al. [7] developed the electrochemical equations to simulate both steady and dynamic behaviors of a two-chambered MFC inoculated with activated sludge and fed with 93.6 mg/L acetate solution. Watson and Logan [8] evaluated the performance of MFCs which exhibited power overshoot when analyzed using common linear sweep voltammetry and fixed resistances methods, and showed that eliminating the power overshoot could be obtained by offering sufficient time for the biofilm to be adjusted to a resistance change by using a single fixed resistance for each separate fed-batch cycle. Kazemi et al. [9] suggested a dynamic one dimensional model for a reverse MFC in which the electrochemical reactions occurred in the cathode instead of anode, and the biofilm formed in the cathode. Ismail and Habeeb [10] developed a steady state, two dimensional model accounting for coupled mass, charge and momentum balances in the biofilm domain for dual chamber MFC with granular activated carbon (GAC) as biofilm bearer for biotreatment of pharmaceutical wastewater. Esfandyari et al. [11,12] proposed a model based on the basic electrochemical equations for both batch and

* Corresponding author.
E-mail address: zismail3@gatech.edu (Z.Z. Ismail).

https://doi.org/10.1016/j.jelechem.2019.02.001
Received 23 October 2018; Received in revised form 31 January 2019; Accepted 1 February 2019
Available online 01 February 2019
1572-6657/

continuous MFC using synthetic lactate-based wastewater.

This study aimed to develop a polarization model for a dual chamber MFC inoculated with non-adapted biomass for simultaneous biotreatment of actual potato chips processing wastewater and electricity generation. The model considered the parameters which may affect the performance of MFC to cause the cell polarization. These parameters included temperature, electrodes geometry and materials dimensions of the MFC, as well as other operating conditions in both anodic and cathodic compartments in addition to the membrane properties.

2. Materials and methods

2.1. Setup and operation of microbial fuel cell

A horizontal dual-chamber MFC constructed of Perspex material was used in this study. Each chamber in the MFC had a total volume of 2000 ml with a working volume of 1900 ml. The anodic and cathodic chambers were separated by a cation exchange membrane (CEM) type CMI-7000 purchased from Membrane International INC., NJ, USA. The effective area of membrane was 14.14 cm^2. Graphite plain electrodes were used in the MFC; each electrode had a surface projected area of 128 cm^2. The anode and cathode electrodes were apart from each other by a distance of 7 cm. The anode chamber was continuously fed with actual potato chips processing wastewater (PCPW) at a rate of 60 ml/h using a peristaltic pump. The real potato chips processing wastewater (PCPW) samples were freshly collected from Salah Al-din Bakery & Pastry Factory located in Tikrit city, Iraq. The average initial concentration of COD in the actual PCPW was 7830 mg/L at pH range of 5.8–6.0, and electrical conductivity of solution was 5210 μS/cm. Fifty ml of anaerobic sludge collected from a local septic tank was used to inoculate the anodic chamber. The biomass was anaerobically enriched and acclimated using peptone-loaded MSM with initial COD concentration of 15,700 mg/L, and then the anodic section was inoculated by this biomass. Then after, the MFC was continuously fueled with actual PCPW. During the system operation phosphate buffer having an electrical conductivity of 12,880 μS/cm was added into the cathode chamber as a catholyte and continuously sparged with an air pump at a rate of 10 ml/min. The MFC was operated at 30 ± 2 °C.

2.2. Analytical methods and electrical measurements

The performance of MFC was evaluated based on the removal efficiency of chemical oxygen demand (COD) and power generation as well. COD concentrations were measured on a daily basis using COD reactor (Type: RD 125, Lovibond, Germany) and COD analyzer (Type: MD 200 COD vario, Lovibond, Germany). The voltage at constant external resistance of 100 Ω was measured at two-min intervals using a voltage data logger (Type: Lascar EL-USB-3, USA). The measured voltages were converted to power according to:

$$P = V_{cell} * I \quad (1)$$

where, P is the power (Watt), I is the current (Amp), and V_{cell} is the cell voltage (V).

2.3. Polarization curve calculations

The polarization curve is a useful tool used for the analysis and description of MFC. A polarization curve is a plot of current density (I) versus electrode potential (E) for a specific electrode-electrolyte combination. It is the basic kinetic law for any electrochemical reaction. Maximum power and current densities can be obtained at the point when the internal and external resistances values are equalized [13]. A digital multimeter (Type: MT1233C, pro'skit, Taiwan) was connected to the anode and cathode electrodes to record voltage with external resistance.

At steady state conditions, the polarization curves were created by changing the external resistances within a range from 5 to 60,000 Ω. Then, the power and current densities were calculated as follows [14]:

$$\text{Power density} = \frac{V_{cell} \times I}{A_{An}} = \frac{(V_{cell})^2}{R_{ext} \times A_{An}} \quad (2)$$

$$\text{Current density} = \frac{V_{cell}}{R_{ext} \times A_{An}} = \frac{I}{R_{ext} \times A_{An}} \quad (3)$$

where:

R_{ext} is the external resistance (Ω).

A_{An} is the surface area of anode (m^2).

3. Model description

In this study, the proposed bio-electrochemical model of MFC focused on the description of the electrode reactions depending on electrode potential and concentrations of reactants/products at the electrode surface as well as the concentrations of chemical and biomass components which were determined by the mass transport and reactions in the biomass and the bulk of liquid. This model was assumed to involve an intracellular mediator and extracellular electron transfer via nanowires or direct contact with the anode for the charge transfer mechanism from a carbon source to the anode, which existed in the reduced and oxidized forms. The model expressed the existence of the attached and suspended microbial populations. Furthermore, the model reflects the influence of numerous parameters including cell geometry, materials, and other operating conditions on MFC performance. The following assumptions were considered to facilitate the model solution [5]:

(1) Ideal mixing, so the carbon source was well distributed in the anodic compartment and substrate gradient in the biofilm was neglected.
(2) The MFC has a non-limiting reaction rate in the cathode compartment.
(3) Multiplicative Monod kinetics was used to describe growth kinetics of anodophilic microorganisms.
(4) Gas transport (e.g. oxygen) through the porous cathode was neglected.
(5) Temperature and pH were maintained constant and fully controlled.

3.1. Material balance

Normally, under anaerobic conditions in the anode chamber, the substrate is oxidized by bacteria. The resulted electrons transfer through the anodic electrode as follows [15]:

$$(CH_2O)_n + nH_2O \rightarrow nCO_2 + 4ne^- + 4nH^+ \quad (4)$$

At anode compartment, the reaction rate of substrate (r_1) at the anode compartment may be calculated using Eq. (5) which was described by [5]:

$$r_1 = k_1^0 \exp\left(\alpha . \frac{F}{R.T} . \eta_{a1}\right) \frac{C_s}{K_s + C_s} . X \quad (5)$$

The reaction of dissolved oxygen reduction in the cathode chamber utilizes the transferred electrons, protons and dissolved oxygen [15]:

$$O_2 + 4e^- + 2H_2O \rightarrow 4OH^- \quad (6)$$

The reaction rate of dissolved oxygen (r_2) at the cathode compartment may be calculated using Eq. (7) according to [7]:

$$r_2 = -k_2^0 \exp\left((\beta - 1) . \frac{F}{R.T} . \eta_{a2}\right) \frac{C_{O2}}{K_{O2} + C_{O2}} \quad (7)$$

It was assumed that both the anode and cathode compartments act as continuously stirred tank reactors. In phase mixture, i.e., all mass-

Table 1
Measured, estimated and assumed parameters and physical constants used in the numerical simulation for MFC models.

Symbol	Description	Value	Unit	Note
F	Faraday's constant	96,485	Coulomb/mol	Constant
R	Gas constant	8.314	J/mol. K	Constant
n	Number of exchange protons/mol of reactant	8	Dimensionless	Constant
T	Temperature	301	K	Constant
k^m	Electrical conductivity of membrane	17	1/Ω.m	Constant
K_{aq}	Electrical conductivity of solution	2	1/Ω.m	Measured
d^m	Thickness of CEM membrane	0.00045	M	Measured
A_m	Area of membrane	0.001414	m^2	Measured
Δ	Thickness of electrode	0.0025	M	Measured
A_{anode}	Area of anode electrode	0.0128	m^2	Measured
A_s	Cross sectional area of solution	0.01	m^2	Measured
d_{cell}	Distance between anode and cathode in the cell	0.07	M	Measured
Va	Volume of anode compartment	0.002	m^3	Measured
Vc	Volume of anode compartment	0.002	m^3	Measured
Y_{ac}	Bacterial yield	0.05	Dimensionless	Assumed
K_d	Decay constant for substrate utilizes	2.314×10^{-7}	1/s	[7]
Qa	Flow rate of fuel feed to anode	$1.667*10^{-8}$	m^3/s	Measured
Qc	Flow rate feeding to cathode compartment	$1.667*10^{-7}$	m^3/s	Measured
C_s^{in}	Inflow substrate concentration	130.5	mol/m^3	Measured
$C_{O2}{}^{in}$	Influent concentration of O_2 of cathode compartment	0.234375	mol/m^3	Measured
X^{in}	Influent concentration of bacteria in anode compartment	0	mol/m^3	Assumed
X	Concentration of bacteria in anode compartment	4.0857	mol/m^3	Estimated
f_x	Reciprocal of wash-out fraction	10	Dimensionless	Assumed
K_s	half velocity rate constant for substrate	0.592	mol/m^3	[7]
K_{O2}	Half velocity rate constant for dissolved oxygen	0.004	mol/m^3	[7]
$C_{CO2}{}^{in}$	Influent concentration of CO_2 of anode compartment	0	mol/m^3	Assumed
$C_H{}^{in}$	Influent concentration of H^+ of anode compartment	0	mol/m^3	Assumed
$C_{OH}{}^{in}$	Influent concentration of OH^- of cathode compartment	0	mol/m^3	Assumed
$C_M{}^{in}$	Influent concentration of M^+ of cathode compartment	0	mol/m^3	Assumed
D^{eff}	Substrate Diffusion Coefficient through the electrode	$1.68727*10^{-6}$	m^2/s	Estimated
V_{OCV}	Cell open circuit voltage	1.039	Volt	Measured
A	The charge transfer coefficient of the anodic reaction	0.18	Dimensionless	Assumed
B	The charge transfer coefficient of the cathodic reaction	0.45	Dimensionless	Assumed
K_1	Rate constant of the anode reaction at standard conditions	$5.75 * 10^{-5}$	mol/m^2. sec	[7]
K_2	Rate constant of the cathode reaction at standard conditions	$9.13 * 10^{-9}$	mol^{12}/m^4. sec	[7]
r_1	Reaction rate for substrate at Anode compartment	$9.2310*10^{-4}$	mol/m^2. sec	Calculated
r_2	Reaction rate for Oxygen at Cathode compartment	$4.7894*10^{-6}$	mol/m^2. sec	Calculated

transport processes, were assumed to be so fast compared to the biochemical and redox reactions, such that the concentrations of all reactants in the bulk solution can be considered equal to those on the surface of electrodes. In addition, carbon dioxide and substrate were assumed not to be diffused into the membrane, and the gas-phase formation by the release of carbon dioxide bubbles was not taken into account. Consequently, the mass balances of the substrate, biomass, H^+, and dissolved CO_2 in the anode compartment were expressed by Eqs. (8), (9), (10) and (11), respectively.

$$V_a\frac{dC_s}{dt} = Q_a(C_s^{in} - C_s) - A_m.\ r_1 \tag{8}$$

$$V_a\frac{dX}{dt} = Q_a\left(\frac{X^{in} - X}{f_x}\right) + A_m.\ Y_{ac}.\ r_1 - V_a.\ K_d.\ X \tag{9}$$

$$V_a\frac{dC_H}{dt} = Q_a(C_H^{in} - C_H) + 4.\ n.\ A_m.\ r_1 \tag{10}$$

$$V_a\frac{dC_{CO_2}}{dt} = Q_a(C_{CO_2}^{in} - C_{CO_2}) + n.\ A_m.\ r_1 \tag{11}$$

In the cathode compartment, the mass balance of dissolved oxygen O_2, hydroxyl ion and cation M^+ were expressed by Eqs. (12), (13), (14), respectively.

$$V_c\frac{dC_{O_2}}{dt} = Q_c(C_{O_2}^{in} - C_{O_2}) + A_m.\ r_2 \tag{12}$$

$$V_c\frac{dC_{OH}}{dt} = Q_c(C_{OH}^{in} - C_{OH}) - 4.\ A_m.\ r_2 \tag{13}$$

$$V_c\frac{dC_M}{dt} = Q_c(C_M^{in} - C_M) + N_M.\ A_m \tag{14}$$

3.2. Voltage and overpotential

The overpotential or polarization can be defined as the losses or the decrease in the actual fuel cell voltage V_{cell} from the equilibrium potential by a series of irreversible losses. Three sources of these losses are illustrated by Picioreanu et al. [16]:

(1) Activation overpotential (η_a), which occurs at the electrode surface and directly related to the rates of electrochemical reactions.
(2) Ohmic overpotential (η_Ω) which defined as the resistance to the flow of ions in the electrolyte and to the electrons flow through the electrode materials.
(3) Concentration overpotential (η_c), related to the mass transfer limitations of chemical species transported to or from the electrode.

Taking into consideration all polarization losses at anode and cathode, the overall cell voltage can be written as follows:

$$V_{cell} = V_{OCV} - (\eta_{a1} + \eta_{c1}) - (\eta_{a2} + \eta_{c2}) - \eta_\Omega \tag{15}$$

where:
V_{cell} = MFC voltage (V).
V_{OCV} = open circuit voltage of the MFC (V).
η_{a1}, η_{a2}, η_{c1}, $\eta_{c2}$and η_Ω are the anodic activation overpotential, cathodic activation overpotential, anodic concentration overpotential,

cathodic concentration overpotential and ohmic overpotential (V) respectively.

The following equations described by Cannarozzo et al. [17]; O'Hayre et al. [18]; and Zeng et al. [7] illustrate the calculations of the entire overpotential:

$$\eta_{a1} = \frac{\ln\left[\frac{r_1(K_s + C_s)}{K_1 . C_s . X}\right]}{\frac{\alpha . F}{R . T}} \quad (16)$$

$$\eta_{a2} = \frac{-\ln\left[\frac{r_2(K_{O2} + C_{O2})}{K_2 . C_{O2}}\right]}{\frac{(\beta - 1) . F}{RT}} \quad (17)$$

The overall ohmic resistances (R_Ω) can be calculated as follows:

$$R_\Omega = \left(\frac{d^m}{k^m} + \frac{d_{cell}}{k_{aq}}\right) i_{cell} \quad (18)$$

$$\eta_\Omega = R_\Omega . i_{cell} \quad (19)$$

$$\eta_{conc} = \frac{RT}{nF} \times \ln \frac{il}{il - i} \quad (20)$$

This model was solved by a routine programming using MATLAB software version (R2017b) at a steady state condition for all equations previously mentioned. All the parameters and constants of are summarized in Table 1.

4. Results and discussions

4.1. COD removal

MFC was continuously operated for 60 days achieving a maximum COD removal efficiency of 99.6% as given in Fig. 1. It is well observed that the profile of COD removal exhibited three phases; fast rate COD removal up to 80% at the first phase until the tenth day of operation, followed by a second phase in which a relatively slower rate of COD removal was observed and a COD removal efficiency of 90% was achieved end of the two weeks of operation. Then after, the MFC almost achieved steady state condition at the 20th day of operation and a complete removal of COD up to more than 99% was observed at third phase. These observations may be attributed to the fact that food processing wastewater as a substrate in MFC is favorable to the microorganisms despite the high organic loading and complex content. The obtained result was relatively higher than 89% COD removal efficiency for potato processing wastewater used as inoculum and substrate in a batch mode MFC system reported by Kiely et al. [19].

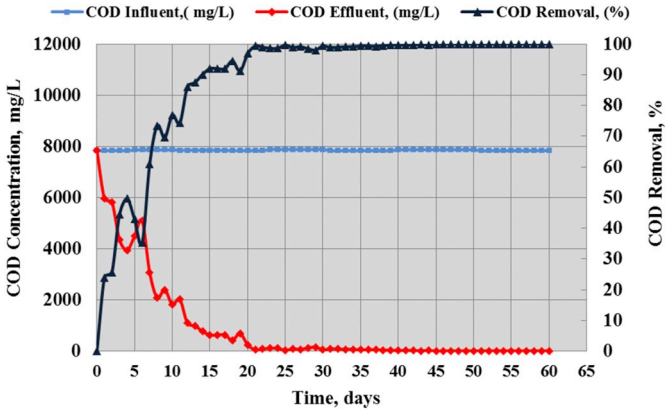

Fig. 1. Profile of COD removal efficiency.

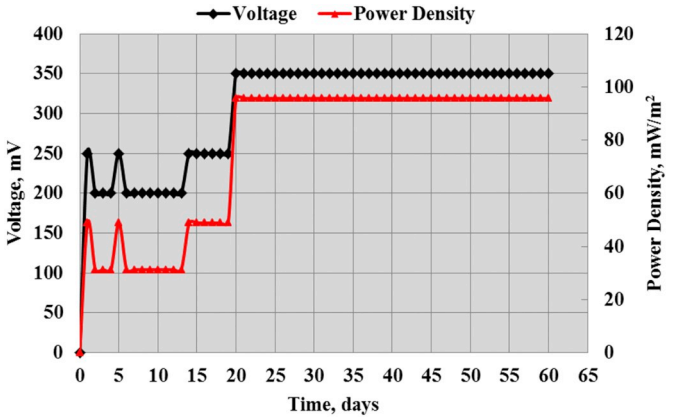

Fig. 2. Profiles of voltage and power density at 100 Ω external resistance.

4.2. Voltage output and electricity generation in MFC

Voltage generation was observed and recorded since the first day of operation. As given in Fig. 2, a relatively margin fluctuation was observed before achieving a steady state conditions. The fluctuation in electricity generation when using actual wastewater was well expected due to the fact that normally the concentration of organic pollutant is not firmly constant. Also, the high organic loading may cause a kind of inhibition to the non-acclimated biomass at the beginning of the operation. However, maximum voltage value of 350 mV and power density value of 95.7 mW/m^2 were obtained through out a closed circuit at 100 Ω after 20 days of continuous operation suggesting that electron transfer was improved due to the efficient oxidation of substrate. The power density observed in this study was comparable to a power density of 90 mW/m^2 at 100 Ω which was previously reported by Mohammed and Ismail [20] for the treatment of slaughterhouse wastewater in MFC system operated in a continuous mode.

4.3. Coulombic efficiency

The Columbic efficiency (CE) is the fraction of the total electron produced and transferred from the anodic electrode over the maximum conceivable electrons produced from the substrate oxidation process. The CE for the system can be calculated as follows [21]:

$$\epsilon_{cb} = \frac{MI}{Fbq\Delta COD} \quad (21)$$

where: F is the Faraday constant which is 96,485 coulomb/mol, M is the oxygen molecular weight, b is a constant which represents the number of electrons exchanged per mole of oxygen, ΔCOD is the difference between the inlet and outlet chemical oxygen demand concentration, (g/L) and q is the flow rate of substrate, (L/s).

The maximum CE value for the MFC was 2.94% obtained at the first day.

However, the CE value of MFC at steady-state conditions was 0.70%. Generally, the CE results were comparatively not high. However, they were greater than CE value of 0.04% for starch processing wastewater reported by Park et al. [22].

As a matter of fact, the CE is not directly related to the power density, since it is not a kinetic parameter. Thus, a low CE can be attributed to low density of anode-respiring microorganisms in the anodic biofilm that caused by a competition for space between bacteria which contributes to the lowering of power density [23].

In addition, COD removal and substrate flowrate are inversely proportional to the CE. The relatively lower CE values with high power densities and high COD removal efficiencies values in the MFC can be attributed to the fact that actual wastewater like actual potato chips processing wastewaters in the anodic chamber have a heterogeneously

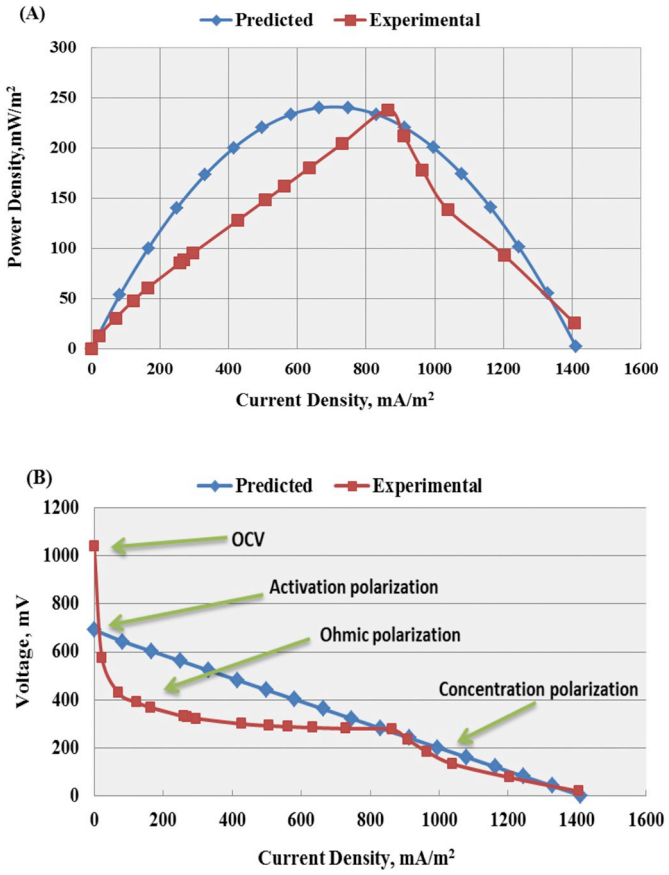

Fig. 3. Predicted and experimental polarization curves for MFC system based on current density against (A) power density, (B) voltage, with polarization regions.

complex chemical composition and comprise of various microbial consortiums in which plentiful biochemical reactions have governed the pathway of bacterial metabolic. Moreover, the consumption of organic substrates in the anodic chamber is a biochemical process depends on microbial consortium, biofilm functioning and growth, as well as the diffusion of oxygen through cation exchange membrane separator to the wastewater in the anodic compartment [24–27].

4.4. Polarization curves and model validation

The results revealed that maximum current and power densities of 862.5 mA/m^2 and 238.1 mW/m^2, respectively were observed at 25 Ω which was the optimum value of internal resistance achieved when the internal resistance met the external resistance (25 Ω) of the system. Thus, these values of maximum current and power densities were relatively higher than those demonstrated by the previously reported studies. Mohammed and Ismail [20] reported 165.22 mW/m^2 and 472 mA/m^2 values for power and current densities, respectively obtained at 40 Ω external resistance from slaughterhouse wastewater treatment in a biocathode-MFC system. Kiely et al. [19] suggested a maximum current density of 217 mW/m^2 for the potato processing wastewater treated in air cathode-MFC system.

Fig. 3 presents the profiles of the predicted and experimental results for current density against power density and voltage, respectively. A significant agreement can be observed between the behavior of predicted and experimental results with relatively high values of coefficient of determination (R^2) of 0.9888, and 0.9197 and 0.9156 between predicted and experimental results of current density, power density, and voltage, respectively. The obvious difference between the curves observed in the activation polarization region can be attributed to the

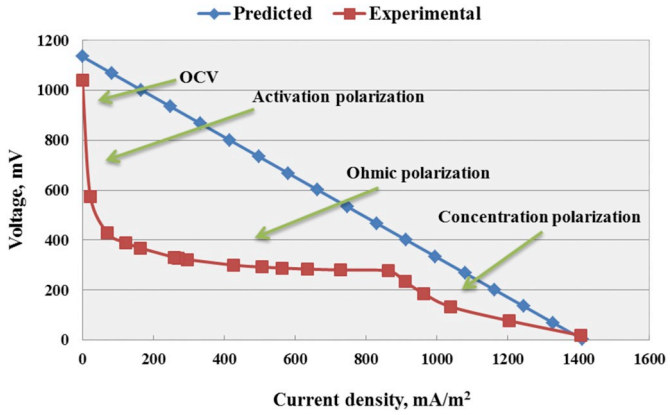

Fig. 4. The experimental and optimum predicted current-voltage profile at different resistances.

fact that the predicted curves did not take into consideration the change of bacterial activity over time. Also, the distribution of microbial populations in the anode biofilm was assumed uniform and to simplify the model, an ideal distribution of the carbon source in anodic chamber with ideal gradient and mixing was considered. However, this difference between the predicted and experimental profiles was well expected due to the complexity of the substrate nature and the bio-electrochemical reactions occurred in the MFC.

Fig. 4 presents a comparison between the predicted and experimental databases of voltages versus current densities were plotted. Fig. 4 shows the highest theoretical amount of energy obtained from an organic substrate if the MFC operates at ideal conditions of voltage generation with very little losses at different external resistances. The results indicated a reasonable similarity between the predicted and experimental profiles curves with coefficient of determination (R^2) of 0.7567.

The highest theoretical amount of energy can be gained from an organic substrate, when the substrate completely oxidized to carbon dioxide with efficient transfer of electrons to the electrode [28].Therefore, the significant difference between the two curves indicated that longer time may be required for the biofilm to be rich with electro-active species, or changes in bacterial respiration rates to increase the energy production [29]. On the other hand, Logan et al. [30] reported that low solution conductivity is known to adversely impact the power generation in microbial fuel cells (MFCs), and often, the real source of wastewater becomes challenging due to its relatively low solution conductivity. However, in this study the average conductivity of the real PCPW was relatively high (5210 μS/cm) compared to other food processing wastewaters [31].

5. Conclusion

This study revealed the validity of using the MFC-system for simultaneous biotreatment of real potato chips processing wastewater (PCPW) and electricity generation. The results demonstrated high removal efficiency of COD up to 99% associated with a relatively significant energy generation at room temperature, which would allow greater simplicity of the system and lower operational costs. Therefore it can be used simply to treat actual potato chips processing wastewater. Also, this study suggested an electrochemical model to describe the performance of the MFC in regard with the predicted data for polarization curve. The model considered the losses occurred in the anodic and cathodic compartments, the membrane and solutions. The results demonstrated high coefficient of determination (R^2) of 0.99, 0.92 and 0.92 for current density, power density, and voltage, respectively. Also, the model predicted the highest theoretical energy which can be obtained in the MFC continuously operated for a relatively long time.

Therefore, this model is very important to provide a clear description of the MFC performance.

Acknowledgement

The authors sincerely acknowledge the staff of Salah Al-din Bakery & Pastry Factory in Tikrit city, Iraq for their support.

References

[1] Y.T. Hung, H.H. Lo, A. Awad, H. Salman, Potato wastewater treatment, Waste Treatment in the Food Processing Industry, 2006, pp. 193–254.
[2] B.E. Logan, B. Hamelers, R. Rozendal, U. Schröder, J. Keller, S. Freguia, K. Rabaey, Microbial fuel cells: methodology and technology, Environ. Sci. Technol. 40 (2006) 5181–5192.
[3] I.S. Han, C.B. Chung, A hybrid model combining a support vector machine with an empirical equation for predicting polarization curves of PEM fuel cells, Int. J. Hydrog. Energy 42 (2017) 7023–7028.
[4] A.A. Kulikovsky, Analysis of Damjanovic´ kinetics of the oxygen reduction reaction: stability, polarization curve and impedance spectra, J. Electroanal. Chem. 738 (2015) 130–137.
[5] A.K. Marcus, C.I. Torres, B.E. Rittmann, Conduction-based modeling of the biofilm anode of a microbial fuel cell, Biotechnol. Bioeng. 98 (2007) 1171–1182.
[6] C. Picioreanu, I.M. Head, K.P. Katuri, M.C. van Loosdrecht, K. Scott, A computational model for biofilm-based microbial fuel cells, Water Res. 41 (2007) 2921–2940.
[7] Y. Zeng, Y.F. Choo, B.H. Kim, P. Wu, Modelling and simulation of two-chamber microbial fuel cell, J. Power Sources 195 (2010) 79–89.
[8] V.J. Watson, B.E. Logan, Analysis of polarization methods for elimination of power overshoot in microbial fuel cells, Electrochem. Commun. 13 (2011) 54–56.
[9] M. Kazemi, D. Biria, H. Rismani-Yazdi, Modelling bio-electrosynthesis in a reverse microbial fuel cell to produce acetate from CO_2 and H_2O, Phys. Chem. Chem. Phys. 17 (2015) 12561–12574.
[10] Z.Z. Ismail, A.A. Habeeb, Experimental and modeling study of simultaneous power generation and pharmaceutical wastewater treatment in microbial fuel cell based on mobilized biofilm bearers, Renew. Energy 101 (2017) 1256–1265.
[11] M. Esfandyari, M.A. Fanaei, R. Gheshlaghi, M.A. Mahdavi, Dynamic modeling of a continuous two-chamber microbial fuel cell with pure culture of Shewanella, Int. J. Hydrog. Energy 42 (2017) 21198–21202.
[12] M. Esfandyari, M.A. Fanaei, R. Gheshlaghi, M.A. Mahdavi, Mathematical modeling of two-chamber batch microbial fuel cell with pure culture of Shewanella, Chem. Eng. Res. Des. 117 (2017) 34–42.
[13] Z.D. Liu, H.R. Li, Effects of bio-and abio-factors on electricity production in a mediatorless microbial fuel cell, Biochem. Eng. J. 36 (2007) 209–214.
[14] H.S. Lee, P. Parameswaran, A. Kato-Marcus, C.I. Torres, B.E. Rittmann, Evaluation of energy-conversion efficiencies in microbial fuel cells (MFCs) utilizing fermentable and non-fermentable substrates, Water Res. 42 (2008) 1501–1510.
[15] I.S. Chang, H.S. Moon, O. Bretschger, J.K. Jang, H.I. Park, K.H. Nealson, B.H. Kim, Electrochemically active bacteria (EAB) and mediator-less microbial fuel cells, J. Microbiol. Biotechnol. 16 (2006) 163–177.
[16] C. Picioreanu, M.C. van Loosdrecht, T.P. Curtis, K. Scott, Model based evaluation of the effect of pH and electrode geometry on microbial fuel cell performance, Bioelectrochemistry 78 (2010) 8–24.
[17] M. Cannarozzo, S. Grosso, G. Agnew, A. Del Borghi, P. Costamagna, Effects of mass transport on the performance of solid oxide fuel cells composite electrodes, J. Fuel Cell Sci. Technol. 4 (2007) 99–106.
[18] R. O'Hayre, S.-W. Cha, W. Colella, F.B. Prinz, Fuel Cell Fundamentals, Wiley & Sons, N.Y, 2009.
[19] P.D. Kiely, R. Cusick, D.F. Call, P.A. Selembo, J.M. Regan, B.E. Logan, Anode microbial communities produced by changing from microbial fuel cell to microbial electrolysis cell operation using two different wastewaters, Bioresour. Technol. 102 (2011) 388–394.
[20] A.J. Mohammed, Z.Z. Ismail, Slaughterhouse wastewater biotreatment associated with bioelectricity generation and nitrogen recovery in hybrid system of microbial fuel cell with aerobic and anoxic bioreactors, Ecol. Eng. 125 (2018) 119–130.
[21] H. Liu, S.A. Cheng, B.E. Logan, Production of electricity from acetate or butyrate using a single chamber microbial fuel cell, Environ. Sci. Technol. 39 (2005) 658–662.
[22] H.S. Park, B.H. Kim, H.S. Kim, H.J. Kim, G.T. Kim, M. Kim, I.S. Chang, Y.K. Park, H.I. Chang, A novel electrochemically active and Fe(III) reducing bacterium phylogenetically related to Clostridium butyricum isolated from a microbial fuel cell, Anaerobe 7 (2001) 297–306.
[23] H.S. Lee, P. Parameswaran, A. Kato-Marcus, C.I. Torres, B.E. Rittmann, Evaluation of energy-conversion efficiencies in microbial fuel cells (MFCs) utilizing fermentable and non-fermentable substrates, Water Res. 42 (2008) 1501–1510.
[24] W. Verstraete, S. Kim, K. Chae, M. Choi, Microbial fuel cells: recent advances, bacterial communities and applications beyond electricity generation, Environ. Energy Resour. 13 (2008) 51–65.
[25] Q. Wen, Y. Wu, D. Cao, L. Zhao, Q. Sun, Electricity generation and modeling of microbial fuel cell from continuous brewery wastewater, Bioresour. Technol. 100 (2009) 4171–4175.
[26] H. Luo, G. Liu, S. Jin, Phenol degradation in microbial fuel cells, Chem. Eng. Natl. Res. Microbiol. J. 147 (2009) 259–264.
[27] C.I. Torres, A.K. Marcus, H.S. Lee, P. Parameswaran, R. Brown, B.E. Rittmann, A kinetic perspective on extracellular electron transfer by anode-respiring bacteria, Appl. Microbiol. Biotechnol. 34 (2010) 3–17.
[28] A.E. Franks, K.P. Nevin, Microbial fuel cells, a current review, Energies 3 (2010) 899–919.
[29] H. Yi, K.P. Nevin, B.C. Kim, A.E. Franks, A. Klimes, L.M. Tender, D.R. Lovley, Selection of a variant of Geobacter sulfurreducens with enhanced capacity for current production in microbial fuel cells, Biosens. Bioelectron. 24 (2009) 3498–3503.
[30] B.E. Logan, E. Zikmund, W. Yang, R. Rossi, K.Y. Kim, P.E. Saikaly, F. Zhang, Impact of ohmic resistance on measured electrode potentials and maximum power production in microbial fuel cells, Environ. Sci. Technol. 52 (2018) 8977–8985.
[31] N.A. Noukeu, I. Gouado, R.J. Priso, D. Ndongo, V.D. Taffouo, S.D. Dibong, G.E. Ekodeck, Characterization of effluent from food processing industries and stillage treatment trial with *Eichhornia crassipes* (Mart.)and *Panicum maximum* (Jacq), Water Resour. Ind. 16 (2016) 1–18.